Cytogenet Genome Res 97:62–67 (2002)

Cytogenetic and Genome Research

The genomic structure, chromosomal localization, and analysis of SIL as a candidate gene for holoprosencephaly

J.D. Karkera,[a] S. Izraeli,[b] E. Roessler,[a] A. Dutra,[c] I. Kirsch,[b] and M. Muenke[a]

[a] Medical Genetics Branch, National Human Genome Research Institute;
[b] Genetics Branch, Center for Cancer Research, National Cancer Institute;
[c] Cytogenetic and Confocal Microscopy Core, National Human Genome Research Institute, National Institutes of Health, Bethesda MD (USA)

Abstract. Holoprosencephaly (HPE) is the most common congenital malformation of the brain and face in humans. In this study we report the analysis of SIL (SCL interrupting locus) as a candidate gene for HPE. Fluorescent in situ hybridization (FISH) analysis using a BAC 246e16 confirmed the assignment of SIL to 1p32. Computational analysis of SIL at the protein level revealed a 73% overall identity between the human and murine proteins. Denaturing high performance liquid chromatography (dHPLC) techniques were used to screen for mutations and these studies identified several common polymorphisms but no disease-associated mutations, suggesting that SIL is not a common factor in HPE pathogenesis in humans.

Holoprosencephaly (HPE) results from an incomplete separation of the primordial single eye field and ventral forebrain into distinct left and right halves. HPE manifests a highly variable phenotype from the severe malformation that leads to cyclopia at one extreme, through a nearly continuous spectrum to simply closely spaced eyes (Muenke and Beachy, 2000; Roessler and Muenke, 2000). The incidence of HPE is 1:10,000–20,000 live births (Roach et al., 1977); however, these estimates do not reflect intrauterine lethality since the true incidence of HPE in utero is 1 in 250 (Matsunaga and Shiota, 1977), making HPE the most common malformation of the brain in humans. The etiology of HPE is incompletely understood, but based on recent studies it is clear that there are many important factors that contribute including human genes and the environment. Mutations in several genes have been identified which can result in HPE in humans, including Sonic Hedgehog (SHH), SIX3, ZIC2, and probably others such as TGIF and PTCH (Roessler and Muenke, 2000; Ming et al., 2002). Thus far, mutations in the human SHH gene are among the most common putative causes of familial HPE, which is consistent with the central role that Shh plays as a ventralizing factor produced by the anterior midline prechordal plate. Consistent with our understanding of the pathogenesis of HPE, all of these genes are active during the early embryological stages of eye field and anterior brain development. Thus genes implicated in developmental programs initiated by Shh in model organisms, such as Sil, themselves become excellent candidates for HPE.

Previous genetic studies have suggested that two transmembrane proteins, namely Patched (Ptc) and Smoothened (Smo) are required for Shh signaling (Chen and Struhl, 1996). When Shh binds to Ptc, Smo accumulates in the membrane in a highly phosphorylated state and activates Shh target genes. Likewise, in the absence of the ligand, Smo is less phosphorylated thereby resulting in inactivation of Shh target genes (Chen and Struhl, 1996; Quirk et al., 1997). Nodal, a putative downstream target of Shh signaling is required for the establishment of the axial midline mesendoderm and later is expressed asymmetrically in

Supported by DIR/NHGRI/NIH.

Received 21 May 2002; manuscript accepted 19 June 2002.

Request reprints from Maximilian Muenke, MD, Medical Genetics Branch
National Human Genome Research, National Institutes Health
Bldg 10/C103, Bethesda MD 20892 (USA); telephone: 301-402-8167
fax: 301-496-7157; e-mail: mmuenke@nhgri.nih.gov

Present address of S.I.: Research Section
Department of Pediatric Heamato-Oncology, Sheba Medical Center
Tel-Hashomer (Israel).

the lateral plate mesoderm. Either loss of appropriate Nodal expression on the left side of the lateral plate mesoderm, or its bilateral expression, results in a randomization of heart looping (Meyers and Martin 1999; Tsukui et al., 1999). There is presently no clear conserved mechanism described in vertebrates to actually break symmetry, however, factors such as Nodal are thought help to establish left-right asymmetry; furthermore, as a factor correlated with "leftness" its asymmetric expression ensures that the process is nonrandom and associated with characteristic organ positioning (Meno et al., 1998; Meyers and Martin, 1999; Tsukui et al., 1999). In the murine *Shh*$^{-/-}$ or *Smo*$^{-/-}$ mutants, Nodal is expressed in the vicinity of the node but is not effectively expressed in the lateral plate mesoderm. This absence of left-sided gene expression is correlated with randomization of heart looping in *Shh*$^{-/-}$ mutants and is even more severe in *Smo*$^{-/-}$ mutants where the heart fails to loop in either direction and remains as a straight linear tube. These results suggest an early role of *Shh* signaling in the control of left-right asymmetry either directly or indirectly through actions impacting on the axial midline (Zhang et al., 2001).

We investigated the human SIL (SCL interrupting locus) gene (Aplan et al., 1991) because the murine *Sil*$^{-/-}$ mutants displayed features compatible with the HPE spectrum including arrest of neural tube closure and lack of midline separation at the anterior end of the cranial folds leading to holoprosencephaly-like defects. In addition, these mutants displayed left-right developmental abnormalities manifested as abnormal cardiac looping. In *Sil*$^{-/-}$ mutant embryos the marker *Shh* displays discontinuous expression accompanied by the lack of *Hfh3* expression in the neural tube fold. Heterozygous *Sil*$^{+/-}$ mice are normal, while homozygous *Sil*$^{-/-}$ mice die in utero at E10.5. Izraeli et. al., also found reduced expression of multiple Shh target genes, despite continued *Shh* expression in the node and the notochord and suggested a role for *Sil* in the propagation of Shh signals (Izraeli et al., 1999, 2001). The exact biochemical role of Sil is still unclear due to the absence of homology to any previously known protein. Interestingly, in *Ptc*$^{-/-}$ and *Ptc*$^{-/-}$ double murine mutants the expression of Shh target genes, such as *Gli*, were markedly reduced suggesting that Sil might be required downstream of Smo in the Shh response pathway (Izraeli et al., 2001).

We hypothesized that a mutation that perturbs the normal function of human SIL might be a risk factor for the development of HPE. Therefore, we decided to study the human SIL gene architecture in detail, to confirm its chromosomal location, and to screen the gene for mutations using denaturing high performance liquid chromatography (dHPLC) in our panel of HPE patients.

Materials and methods

Patients and DNA preparation

DNA samples of patients with HPE were collected by informed consent according to the guidelines of the Institutional Review Board of the NHGRI. DNA was isolated from blood or lymhoblastoid cell lines by standard protocols. A total of 83 probands with familial HPE were chosen for dHPLC screening; this panel is known to be representative of the full spectrum of HPE severity. No patients with laterality phenotypes were available for a similar analysis.

Computational analysis of DNA and protein sequences

Unpublished data (I.K.) pertaining to the genomic organization of SIL was further confirmed by nucleotide homology searches in the public database using the BLASTN program (http://www.ncbi.nlm.nih.gov/blast). The compiled data reflecting the gene structure of all 18 exons were then submitted to GenBank. MultiAlign software (http://www.toulouse.inra.fr/multalin.html) was used for protein homology searches between human and murine SIL. Putative structural motifs were analyzed by PFAM (http://www.sanger.ac.uk/Software/Pfam/search.shtml) and ProfileScan (http://www.isrec.isb-sib.ch/cgi-bin/).

Fluorescent in situ hybridization (FISH) analysis

Slides with normal chromosome metaphase spreads were incubated for 1 h at 37°C in 2× SSC (0.3 M NaCl and 0.3 M sodium citrate) and then dehydrated sequentially in 70%, 80%, and 90% ethanol. Chromosomal DNA was denatured in 70% formamide, 2× SSC for 2 min at 72°C followed by dehydration in ethanol washes of 70%, 80%, 90%, and 100%. FISH was performed with the BAC probe 246e16 (Incyte Genomics, MO) labeled with digoxigenin-11-dUTP by nick translation (Boehringer Mannheim, IN) and ethanol precipitated in the presence of 50× Cot-1 human DNA (Lichter et al., 1988). The DNA pellet was resuspended to a final concentration of 25 ng/ml. The hybridization and the post-hybridization step were performed as described earlier (Pack et. al., 1999). Slides were counterstained with DAPI, 250 ng/µl (Boehringer Mannheim, IN) with Antifade. Hybridization signals were scored using a Zeiss Axiophot epifluorescence microscope (Zeiss, NY) and the two-color image was captured on a Photometric charge-coupled device camera (Photometrics, AZ) using IP Lab image software (Signal Analytics, VA).

Denaturing high performance liquid chromatography (dHPLC) screening

Amplification of genomic DNA was performed in a 30 µl reaction volume, using 60–100 ng DNA template, 50 µM dNTP, 0.25 µM of each primer, 3 µl of 10× PCR Amplification buffer (Gibco, MD), 1.5 µl 10× Enhancer buffer (Invitrogen, CA), 0.9 µl of 50 mM $MgSO_4$, and 1 U AmpliTaq (Perkin Elmer, CA). All reactions were performed using a PTC-225 thermocycler (MJ Research, MA). Primer pairs and their respective annealing temperatures are described in Table 1. Typical PCR cycling parameters were 95°C for 4 min followed by 30 cycles at 95°C for 30 s, annealing at the indicated temperatures for 30 s, extension at 72°C for 1 min, culminating in a final step of 72°C for 5 min. One half of the PCR product was used for dHPLC analysis and the other half was retained for direct DNA sequencing.

The dHPLC was performed on a ProStar helix dHPLC system (Varian, CA). In order to enhance heteroduplex formation, the PCR products were denatured at 95°C for 5 min followed by gradual cooling to 60°C over 15 min (1°C/30 sec). The PCR product was automatically injected onto a Helix column and eluted with a linear gradient of buffers A and B (Varian, A: 100 mM triethylamine acetate [pH 7], 0.1 mM EDTA, and B: 100 mM triethylamine acetate [pH 7], 0.1 mM EDTA, 25% (*v/v*) acetonitrile) at a constant rate of 0.9 ml/min. Each sample was analyzed at the melting temperature (T_m) determined by using the dHPLCMelt software (http://insertion.stanford.edu/melt.html). In some instances, two different temperatures were used to enhance the sensitivity of screening. Heterozygous profiles were identified by visual inspection of the chromatograms on the basis of the appearance of additional earlier eluting peaks. Corresponding profiles for the same amplicons, which exhibited only a single peak, could be demonstrated to be homozygous and normal in sequence (data not shown).

Direct DNA sequencing

Amplicons displaying heterozygous profiles were purified using a Qiagen PCR purification kit (Qiagen, CA) and bi-directionally sequenced using the BigDye™ terminator cycle sequencing kit according to the manufacturer's protocol (Applied Biosystems, CA). Sequencing reactions were analyzed on an ABI 377 automated sequencer.

Nomenclature

Gene mutation nomenclature used in this study follows the recommendations of den Dunnen and Antonarakis (2001). Gene symbols are those following the recommendations of the HUGO Gene Nomenclature Committee (http://www.gene.ucl.ac.uk).

Table 1. Primers for SIL mutational analysis

Exon	Primer	T (°C) (PCR)	Size (bp)	GenBank Accession no.	T_m (°C) (dHPLC)
1	5'GTGTTTGCCTCAGTTCCCG 3'		163/		
	5'TCTCAAGGGGAAACCAGGAGCACA 3'	58	5'UTR	AF349640	64
2	5'CTGATTTTTGTATTTTTGGTAGAACG 3'		252/		
	5'AGCTAACTTCATCAACTCACCAGAC 3'	51	5'UTR	AF349641	56/61
3	5'AATTCTTTAGGATACTGAGGATTTGG 3'				
	5'CCTTCCCAAGTTATGTGAAAAGC 3'	52	154	AF349642	54
4	5'CCAAGTTTGCTATTCCTTGTGCT 3'				
	5'CTCTTGTTTATACTGGCTTGATTTGA 3'	51	203	AF349643	56
5	5'GGAGGTTTTTTTAAGATATGAGGTC 3'				
	5'TTACAGGCGTGAGCACTGGTC 3'	51	212	AF349644	57
6	5'GCTGTTATTTTTGTTCTACAGATGAAG 3'				
	5'TCAAGTTGTCAATGAATCGCACC 3'	51	231	AF349645	57
7	5'CTTTGGCGATATGGGCACATTTC 3'				
	5'ACTGGACAATTCTTTCACATTACATGG 3'	55	392	AF349646	58
8	5'TGTCTTCTGTTTAGATATCTTACCATGG 3'				
	5'ACATTTGAACATTTGGCTGATAAGG 3'	51	148	AF349647	54
9	5'GCCATACGTCTACTTTGTTATCTTAGG 3'				
	5'GGGAAAGGATCGAAATAAAGTACTAC 3'	51	225	AF349648	54
10	5'GTTATTTGAGTGTCATCATGTTATCCTC 3'				
	5'ACCCTAAACAGTCACTAATGTACTAGAC 3'	51	256	AF349649	55
11	5'CCGGATCTAAGCTTATCGATTTC 3'				
	5'AAACACACACATAATAACAAAAAGATC 3'	52	237	AF349650	57
12	5'GGTCTCCCCTTCTATTCTTTAGG 3'				
	5'GTCTCTAACCACAAAAGTGAATGC 3'	51	179	AF349651	57
13A	5'GGAAATACTGGGTCTGAGGAAAG 3'				
	5'TTGTGAACAGTAAGATGGCAG 3'	55	632		58
13B	5'CCAGGAACAGTATTAAACCATCTTC 3'			AF349652	
	5'CCTGTGCCTGAAGTAGTCTTAGC 3'	55	471		59
14	5'TGATTACTTCCCTGTCAGTTTAAAG 3'				
	5'AAACTGAAATTACCTGTGCTCAC 3'	51	224	AF349653	54/59
15	5'AATTATTTAACCTCCAGGTGCTAGC 3'				
	5'CAAAGAGACCTTACTTGGATACAG 3'	55	263	AF349654	56
16	5'CACATTATATATCCTTCCCAGCAGC 3'				
	5'TGCTCTACATTTCTTACCAATAAATC 3'	55	253	AF349655	54/59
17	5'ACCACCACACCCAGCCCTAAC 3'				
	5'AAAAGTTACCTGGCGTGATCC 3'	58	328	AF349656	57
18A	5'AATGATGGCTTACTACTTTGTGTC 3'				58
	5'GCTGGCTTTTCAGTCAACTGC 3'	55	600		
18B	5'GAACCTCCCGACAATGCAGATAG 3'			AF349657	
	5'GCTACCAAGAAACAGTGACTCCAG 3'	55	407		58

Results

The BLAST program (NCBI) was used to confirm the gene architecture and establish additional sequence information from the limited initial intron-exon sequence information available (characterized by S.I. and I. K.) facilitating the primer designing process (Table 1). SIL consists of 18 exons wherein the coding region starts from the third exon, with a predicted open reading frame of 3861 nucleotides that encodes 1287 amino acid residues. The nucleotide sequence analysis of the coding region between the human and mouse SIL using MultiAlign software revealed an overall homology of 81%. The amino acid sequence alignment of the human and the mouse SIL displayed an overall identity of 73%. The protein pattern and domain prediction software detected the presence of a putative nuclear localization signal motif KKKTH (residue no. 979–983) and the presence of a cysteine-terminal domain (residue no. 601–702) interestingly sharing a weak homology (N-score ~6.7) to the carboxyl terminal domain in TGF-β (Fig. 1). The chromosome location of the SIL gene was determined to be chromosome 1p32 by FISH analysis (Fig. 2). No signal was seen on any other chromosome in the 20 normal metaphase cells examined.

The dHPLC analysis was performed at the dHPLCmelt recommended temperature(s) as shown in Table 1. All 83 samples with homozygous wild type sequences were correctly identified at the recommended temperature for all the exons. The GC content of amplicons spanning exon 2, 14, and 16 were high at one particular region and thus the dHPLC analysis was repeated at a raised temperature to make it more sensitive in detecting heteroduplexes.

Fig. 1. Protein alignment of human and murine SIL. Identical amino acids between the species are represented by dots; the variable amino acids are shown in red, dash lines are gaps introduced to maximize the alignment. The nuclear localization signal KKKTH (residue no. 979–983) is boxed, and cysteine-terminal domain similar to TGF-β (residue no. 601–702) is depicted by a line above the sequences.

Fig. 2. FISH analysis of SIL. (A) The hybridization of BAC 246e16 containing the SIL gene to chromosome 1p32 is indicated by the red dots. (B) Same metaphase as Fig. 2A with DAPI banding, arrows indicating chromosome 1.

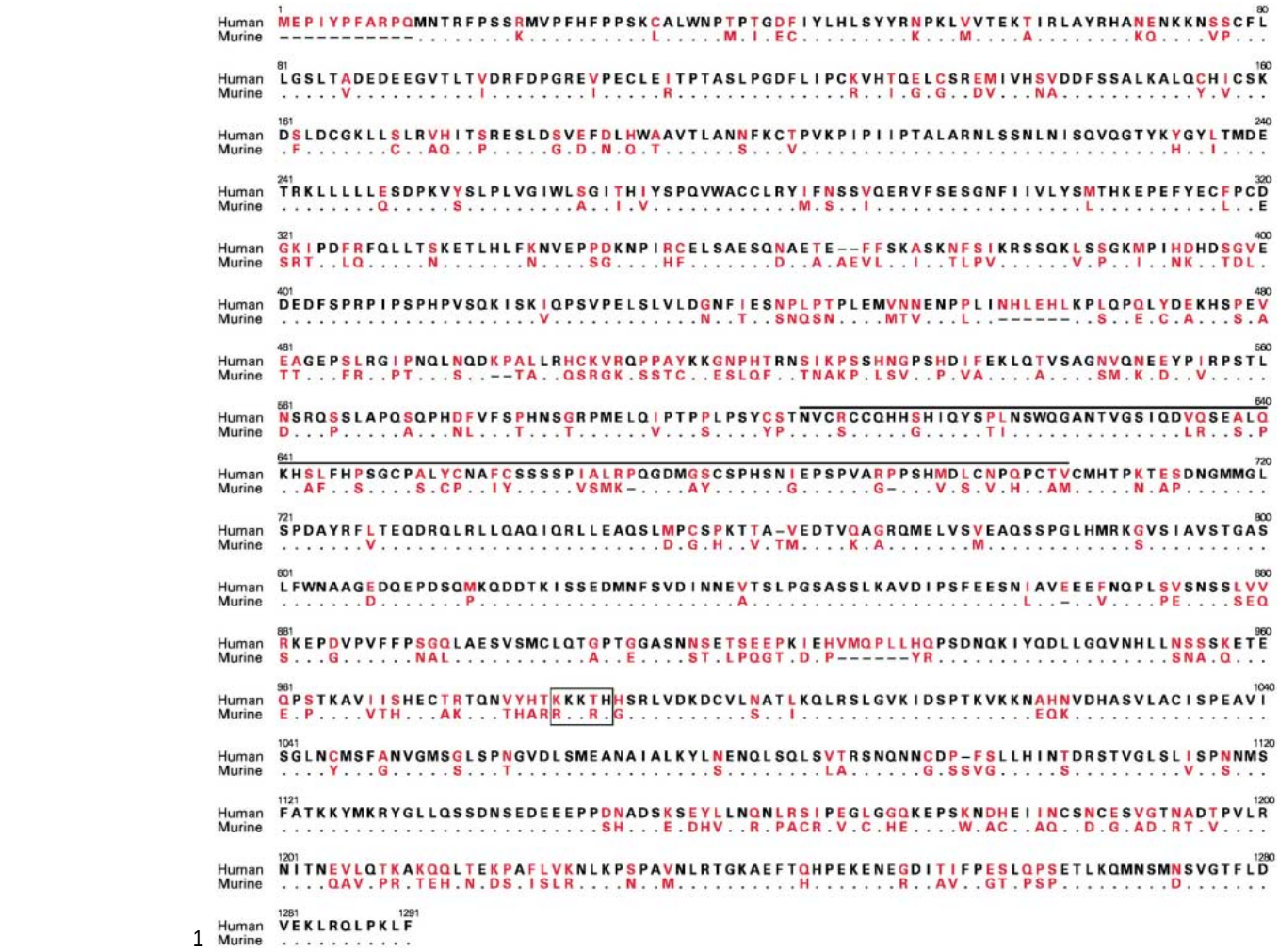
Human MEPIYPFARPQMNTRFPSSRMVPFHFPPSKCALWNPTPTGDFIYLHLSYYRNPKLVVTEKTIRLAYRHANENKKNSSCFL
Murine ----------.....K.....L.....M.I.EC.....K...M....A.....KQ....VP...
Human LGSLTADEDEEGVTLTVDRFDPGREVPECLEITPTASLPGDFLIPCKVHTQELCSREMIVHSVDDFSSALKALQCHICSK
Murine .....V.....I.....I.....R.....R..I.G.G..DV...NA.....Y.V...
Human DSLDCGKLLSLRVHITSRESLDSVEFDLHWAAVTLANNFKCTPVKPIPIIPTALARNLSSNLNISQVQGTYKYGYLTMDE
Murine .F.....C..AQ..P.....G.D.N.Q.T.....S...V.....H..I....
Human TRKLLLLLESDPKVYSLPLVGIWLSGITHIYSPQVWACCLRYIFNSSVQERVFSESGNFIIVLYSMTHKEPEFYECFPCD
Murine .....Q.....S.....A..I.V.....M.S..I.....L.....L..E
Human GKIPDFRFQLLTSKETLHLFKNVEPPDKNPIRCELSAESQNAETE--FFSKASKNFSIKRSSQKLSSGKMPIHDHDSGVE
Murine SRT..LQ.....N.....N....SG....HF.....D..A.AEVL..I..TLPV.....V.P..I..NK..TDL.
Human DEDFSPRPIPSPHPVSQKISKIQPSVPELSLVLDGNFIESNPLPTPLEMVNNENPPLINHLEHLKPLQPQLYDEKHSPEV
Murine .....V.....N..T..SNQSN....MTV...L..------..S..E.C.A...S.A
Human EAGEPSLRGIPNQLNQDKPALLRHCKVRQPPAYKKGNPHTRNSIKPSSHNGPSHDIFEKLQTVSAGNVQNEEYPIRPSTL
Murine TT...FR..PT...S..--TA..QSRGK.SSTC..ESLQF..TNAKP.LSV..P.VA....A....SM.K.D..V.....
Human NSRQSSLAPQSQPHDFVFSPHNSGRPMELQIPTPPLPSYCSTNVCRCCQHHSHIQYSPLNSWQGANTVGSIQDVQSEALQ
Murine D...P.....A...NL...T...T.....V...S....YP....S.....G.....TI.....LR..S.P
Human KHSLFHPSGCPALYCNAFCSSSSPIALRPQGDMGSCSPHSNIEPSPVARPPSHMDLCNPQPCTVCMHTPKTESDNGMMGL
Murine ..AF..S....S.CP..IY.....VSMK-....AY.....G.....G-...V.S.V.H..AM.....N.AP.....
Human SPDAYRFLTEQDRQLRLLQAQIQRLLEAQSLMPCSPKTTA-VEDTVQAGRQMELVSVEAQSSPGLHMRKGVSIAVSTGAS
Murine .....V.....D.G.H..V.TM....K.A.....M.....S.....
Human LFWNAAGEDQEPDSQMKQDDTKISSEDMNFSVDINNEVTSLPGSASSLKAVDIPSFEESNIAVEEEFNQPLSVSNSSLVV
Murine .....D.....P.....A.....L...-..V....PE....SEQ
Human RKEPDVPVFFPSGQLAESVSMCLQTGPTGGASNNSETSEEPKIEHVMQPLLHQPSDNQKIYQDLLGQVNHLLNSSSKETE
Murine S...G.....NAL.....A..E....ST.LPQGT.D.P------YR.....SNA.Q...
Human QPSTKAVIISHECTRTQNVYHTKKKTHHSRLVDKDCVLNATLKQLRSLGVKIDSPTKVKKNAHNVDHASVLACISPEAVI
Murine E.P....VTH...AK...THARR..R.G.....S..I.....EQK.....
Human SGLNCMSFANVGMSGLSPNGVDLSMEANAIALKYLNENQLSQLSVTRSNQNNCDP-FSLLHINTDRSTVGLSLISPNNMS
Murine ....Y...G.....S...T.....S.....LA.....G.SSVG.....S.....V..S...
Human FATKKYMKRYGLLQSSDNSEDEEEPPDNADSKSEYLLNQNLRSIPEGLGGQKEPSKNDHEIINCSNCESVGTNADTPVLR
Murine .....SH...E.DHV..R.PACR.V.C.HE....W.AC..AQ..D.G.AD.RT.V....
Human NITNEVLQTKAKQQLTEKPAFLVKNLKPSPAVNLRTGKAEFTQHPEKENEGDITIFPESLQPSETLKQMNSMNSVGTFLD
Murine ....QAV.PR.TEH.N.DS.ISLR....N..M.....H.....R..AV..GT.PSP.....D.....
Human VEKLRQLPKLF
Murine .....

1


A

2

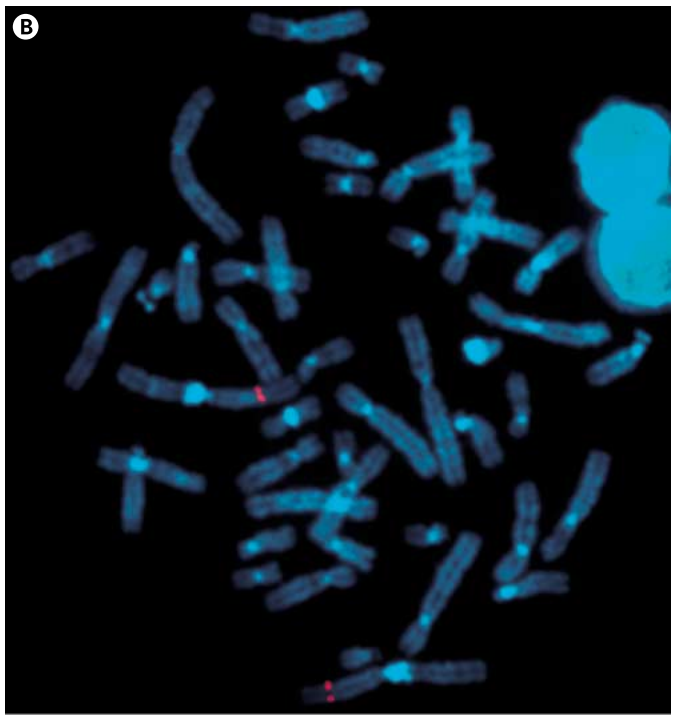
B

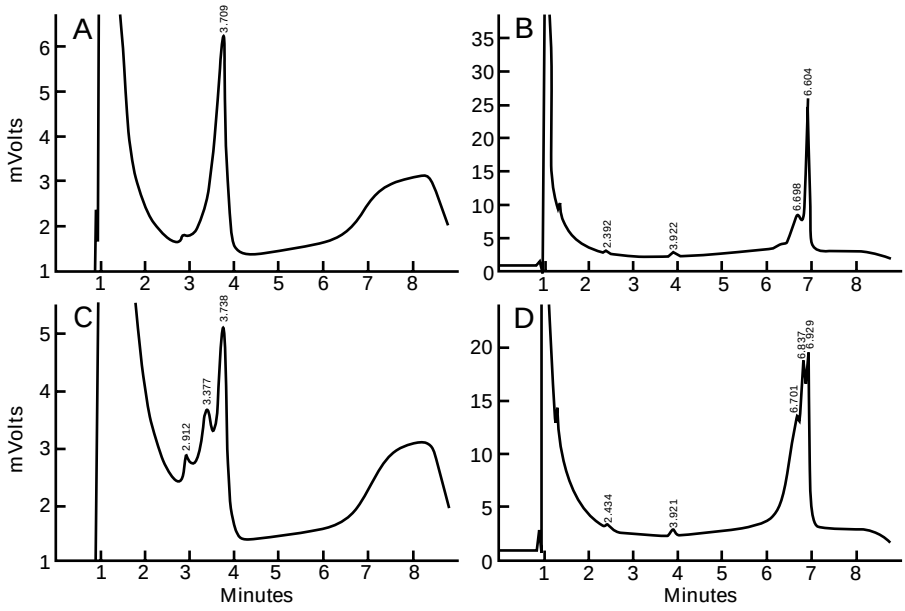

Fig. 3. Examples of selected dHPLC chromatograms of SIL variants. Panels (A), and (C) represent exon 7 containing a 392-bp amplicon analyzed at 58°C wherein Panel (A) represents the wild type and Panel (C) exhibits T→A in the intron region. Panels (B), and (D) represent exon 13A containing a 632-bp amplicon analyzed at 58°C wherein Panel (B) depicts wild type and Panel (D) displays A→T in the intron region.

Table 2. Sequence variations in SIL

Exon	Nucleotide change[a]	Amino acid change	Detections[b]
5	257C→T (homozygous)	Ala→Val	Introduces an *Acc*I R.E. site
7	IVS 7-21T→A (heterozygous)	5' intron region	No R.E. site
13	IVS 13-53A→T (heterozygous)	5' intron region	Abolishes an *Acc*I R.E. site
17	2874G→A (heterozygous)	Pro→Arg	Introduces an *Afl*III R.E. site

[a] IVS: intervening sequence.
[b] R.E.: restriction endonuclease.

Four different heterozygous sequence variations were identified in human SIL (Table. 2); however, none were unique to HPE patients. The first homozygous change in exon 5, 257C→T, predicts an A86V mutation and this sequence change introduces an *Acc*I restriction site. The two intron variations detected were present in exon 7 (IVS 7-21T→A) and exon 13 (IVS 13-53A→T). Examples of heteroduplex detection in exons 7 and 13A are shown in Fig. 3. The sequence variation in exon 7 produced a consistent elution profile but in other cases (not shown) distinct sequence variations with a given amplicon produced different characteristic elution profiles. The fourth heterozygous sequence variation, 2874G→A, predicts a substitution P1015R encoded by exon 17 which introduces an *Afl*III restriction site. Over 200 normal chromosomes were screened either by restriction fragment length polymorphisim or by dHPLC for each of the mutations detected in SIL. All the nucleotide variations detected in SIL were also found to be present in the normal control samples.

Discussion

Animal models of brain development have been successfully applied to further our understanding the pathogenetic mechanism of HPE in humans. *Sil*$^{-/-}$ mutants display severe anterior midline neural-tube defects, abnormalities in left-right axis development, holoprosencephaly-like features, and are embryonic lethal (Izraeli et al., 1999). Furthermore, discontinuous expression of *Shh* and lack of *Hfh3* in the notochord and reduced expression of multiple Shh target genes suggested that *Sil* deserved to be examined as an HPE candidate gene. In this study, we investigated the sequence variations of SIL in HPE and found no evidence for its role as a common genetic determinant of this disorder in our panel of samples.

Sil$^{-/-}$ murine mutants display a lack of midline separation at the anterior end of the cranial folds resulting in holoprosencephaly-like defects and these embryos ultimately die in utero while the heterozygous mice have no distinct phenotype. Since all of our clinical samples were obtained from live-born infants, it appears likely that our failure to find evidence for a role for SIL in HPE results, in part, from the fact that the phenotype may be autosomal recessive lethal in both mice and humans.

The utilization of a high-throughput approach to mutation screening by dHPLC methodology is extremely sensitive, rapid, and very cost-effective as compared to the traditional single-strand conformation polymorphism (SSCP). Even though our mutation screening did not suggest loss or gain of function of SIL as a common denominator of HPE in humans, nonetheless, we cannot formally exclude the possibility that rare cases could be caused by this mechanism.

The bilateral expression of *Nodal*, *Leftb*, and *Pitx2*, in the lateral plate mesoderm of *Sil*$^{-/-}$ murine mutants could be attributed to a defective midline barrier, which allows the spread of the left-right signaling cascade across the midline (Izraeli et al., 1999; Bisgrove et al., 2000). Similar observations have been made in zebrafish *ntl* and *flh* mutants (Rebagliati et al., 1998) where the generation of the midline barrier and not the generation of left-right signals at the node are affected (Bisgrove et al., 2000). In the zebrafish, *cyc* (nodal) is critical for the regulation of *lft1, lft2*, and *pitx2,* and is required for the establishment of cardiac laterality (Yost, 1999). These findings suggest that the genes involved in establishing or maintaining the anterior midline barrier can be associated with the development of brain, heart, and gut asymmetries (Bisgrove et al., 2000).

Targeted mutation of *Ebaf* (Meno et al., 1998) and *Pitx2* (Kitamura et al., 1999) has demonstrated the importance of these genes in left-right axis formation (Casey and Hackett, 2000). Since *Ptc*$^{-/-}$ murine mutants exhibit left-right development abnormalities associated with a lack of *Ebaf* expression and bilateral expression of *Nodal*, *Leftb*, and *Pitx2*, we propose that SIL might be an excellent candidate gene to study in laterality patients. Furthermore, the defect appears to be related to Shh signaling since *Ptch* and *Gli* expression are both reduced in *Sil*$^{-/-}$ embryos. Therefore, the identification of the gene structure and our strategy to analyze the human SIL gene should facilitate the examination of laterality phenotypes.

Acknowledgements

We thank all of the families for participating in these studies, and the Don and Linda Carter Foundation for their support.

References

Aplan PD, Lombardi DP, Kirsch IR: Structural characterization of SIL, a gene frequently disrupted in T-cell acute lymphoblastic leukemia. Mol Cell Biol 11:5462–5469 (1991).

Bisgrove BW, Essner JJ, Yost J: Multiple pathways in the midline regulate concordant brain, heart and gut left-right asymmetry. Development 127:3567–3579 (2000).

Casey B, Hacket BP: Left-right axis malformations in man and mouse. Curr Opin Genet Dev 3:257–261 (2000).

Chen Y, Struhl G: Dual roles for patched in sequestering and transducing hedgehog. Cell 87:553–563 (1996).

den Dunnen JT, Antonarakis SE: Nomenclature for the description of human sequence variations. Hum Genet 109:121–124 (2001).

Izraeli S, Lowe LA, Bertness VL, Campaner S, Hahn H, Kirsch IR, Kuehn M: Genetic evidence that Sil is required for the sonic hedgehog response pathway. Genesis 31:72–77 (2001).

Izraeli S, Lowe LA, Bertness VL, Good DJ, Dorward DW, Kirsch IR, Kuehn M: The SIL gene is required for mouse embryonic axial development and left-right specification. Nature 399:691–694 (1999).

Kitamura K, Miura H, Miyagawa-Tomita S, Yanazawa M, Katoh-Fukui Y, Suzucki R, Ohuchi H, Suehiro A, Motegi Y, Nakahara Y, Kondo S, Yokoyama M: Mouse Pitx2 deficiency leads to anomalies of the ventral body wall, heart, extra-and periocular mesoderm and right pulmonary isomerism. Development 126:5749–5758 (1999).

Lichter P, Cremer T, Borden J, Manuelidis L, Ward DC: Delineation of human chromosomes in metaphase and interphase cells by in situ suppression hybridization using recombinant DNA libraries. Hum Genet 80:224–234 (1988).

Matsunaga E, Shiota K: Holoprosencephaly in human embryos: epidemiologic studies of 150 cases. Teratology 16:261–272 (1977).

Meno C, Shimono A, Saijoh Y, Yashiro K, Mochida K, Ohishi S, Noji S, Kondoh H, Hamada H: Lefty-1 is required for left-right determination as a regulator of Lefty-2 and Nodal. Cell 94:287–297 (1998).

Meyers EN, Martin GR: Differences in left-right axis pathways in mouse and chick: functions of FGF8 and SHH. Science 285:403–406 (1999).

Ming JE, Kaupas ME, Roessler E, Brunner HG, Golhi M, Tekin M, Scration RF, Sujansky E, Bale SJ, Muenke M: Mutations in PATCHED-1, the receptor for SONIC HEDGEHOG are associated with holoprosencephaly. Hum Genet 110:297–301 (2002).

Muenke M, Beachy PA: Holoprosencephaly, in Schriver et al (eds): Metabolic Molecular Basis of Inherited Disease, Chapter 250, pp 6203–6230 (McGraw-Hill, New York 2000).

Pack SD, Karkera JD, Zhuang Z, Pack ED, Balan KV, Hwu P, Park W-S, Phan T, Ault DO, Glaser M, Liotta L, Detera-Wadleigh SD, Wadleigh RG: Molecular cytogenetic fingerprinting of esophageal squamous cell carcinoma by comparative genomic hybridization reveals a consistent pattern of chromosomal alterations. Genes Chrom Cancer 25: 160–168 (1999).

Quirk J, van den Heuvel M, Henrique D, Margio V, Jones TA, Tabin C, Ingham PW: The smoothened gene and hedgehog signal transduction in Drosophila and vertebrate development. Cold Spring Harb Symp Quant Biol 62:217–226 (1997).

Rebagliati MR, Toyama R, Haffter P, Dawid IB: Zebrafish nodal-related genes are implicated in axial patterning and establishing left-right asymmetry. Dev Biol 199:261–272 (1998).

Roach E, DeMyer W, Connelly PM, Palmer C, Merritt AD: Holoprosencephaly: birth data, genetic and demographic analyses of 30 families. Birth Defects 11:294–331 (1977).

Roessler E, Muenke M: The structure and function of genes causing human holoprosencephaly. Gene Function Disease 1:1–14 (2000).

Tsukui T, Capdevila J, Tamura K, Ruiz-Lozano P, Rodriguez-Esteban C, Yonei-Tamura S, Magallon J, Chandraratna RA, Chien K, Blumberg B: Multiple left-right asymmetry defects in Shh$^{-/-}$ mutant mice unveil a convergence in the control of lefty-1. Proc natl Acad Sci, USA 96:11376–11381 (1999).

Yost HJ: Diverse initiation in a conserved left-right pathway? Curr Opin Genet Dev 9:422–426 (1999).

Zhang XM, Ramalho-Santos M, McMhoan AP: Smoothened mutants reveal redundant roles for Shh and Ihh signaling including regulation of L/R asymmetry by the mouse node. Cell 105:781–792 (2001).